Modeling semiconductor optical devices

G. E. Sartoris

Technikum Winterthur, Postfach Winterthur, 8401, Switzerland
guido@pfi.ibk.baum.ethz.ch

ABSTRACT

In this article, numerical methods for modeling photonic devices having coupled electrical and optical fields are presented. The governing equations characterizing the problem are presented as well as algorithms for computing numerical solutions. The coupling between the electrical and optical field is introduced as a generation or recombination term for the drift-diffusion model. The numerical results of a semiconductor laser device which is under investigation for use in all-optical communications systems are also given.

Keywords: Device modeling, photonic devices, semiconductor lasers.

INTRODUCTION

Semiconductor modeling plays an important role in the industrial development cycle. Although for generic semiconductor devices several modeling tools are nowadays available, for photonic devices this is generally not the case. Peculiar to these devices is the coupling between electrical and optical fields which plays an important role in the device behavior. The treatment of this coupling and the computation of numerical solutions may be considered a complex task, also because a global modeling concept it is not available. In this work this problem is addressed and a method for computing a certain class of photonic devices is presented as implemented in the program NM Seses (SEmiconductor Sensor and actuator Simulation).

The electrical behavior of a semiconductor device may be well characterized by computing the electrical fields with the classical drift-diffusion model from the electric potential, electron and hole densities. More complex is the approximation and computation of the optical fields since they strongly depend on the class of problem to be modeled. Here, a standard solution is not available and for different classes of devices, different numerical algorithms must be implemented. In the present work, the optical fields are computed as the quasi-TE or quasi-TM modes of two-dimensional dielectric waveguides. These modes are obtained by solving the scalar Helmholtz problems for one of the transversal components of the electric or the magnetic field. Once the governing equations for the electrical and the optical fields are specified, it is possible to define the coupling between these fields quite generally with the introduction of recombination models, as for example when stimulated recombination or absorption of light is present. This step may be considered quite simple, but the specification of the model's parameters generally requires complex experimental investigations.

In the present article numerical results for a semiconductor laser device being investigated for use in all-optical communication systems are reported. The device consists of a planar dielectric rib waveguide and a hetero p-i-n laser diode as depicted in Fig. 1. For clarity, the figure only shows a small section of the real device which is actually much longer and is only a single component on a chip developed for switching optical signals. Because the lateral dimensions of the laser device are small compared with the longitudinal length, the laser device can be well characterized by studying a single two-dimensional section.

GOVERNING EQUATIONS FOR ELECTRICAL FIELDS

We use here the classical unstationary drift-diffusion model [9], [13] as the governing equations for the electric potential ψ and the electron n and hole p densities. The model consists of the partial differential equations

$$\begin{aligned}
\vec{\nabla}(\epsilon\vec{\nabla}\psi) &= q(n-p-C)\,, \\
-q\frac{\partial n}{\partial t}+\vec{\nabla}\vec{J}_n &= qR(n,p)\,, \\
\vec{J}_n &= qD_n n_{in} e^{\psi/V_T}\vec{\nabla}(e^{-\psi/V_T}n/n_{in})\,, \\
q\frac{\partial p}{\partial t}+\vec{\nabla}\vec{J}_p &= -qR(n,p)\,, \\
\vec{J}_p &= -qD_p n_{ip} e^{-\psi/V_T}\vec{\nabla}(e^{\psi/V_T}p/n_{ip})\,,
\end{aligned} \tag{1}$$

with ϵ the dielectric permittivity, C the bulk charge, $V_T \approx 0.025V$ the thermal voltage, $R(n,p)$ the recombination rate and $D_{n,p}$ the diffusion coefficients.

Because most semiconductor optical devices are made of heterogeneous materials, the modeling process starts with a correct characterization of the bandshapes at thermodynamic equilibrium when the currents $\vec{J}_{n,p}$ are

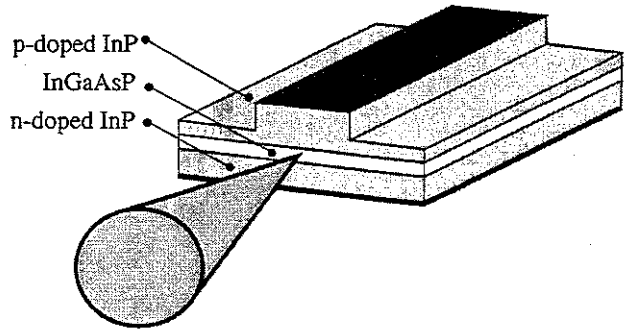

Figure 1: A semiconductor laser device forming a rib-waveguide and composed of three layers: (top) p-doped InP, (middle) intrinsic InGaAsP, (bottom) n-doped InP. Electrical contacts are deposited on the top and bottom of the device. For the steady state solutions presented in the following, the laser diode is forward biased by 1.4 V.

null. This is achieved by defining the intrinsic density n_i to be a space dependent entity. However, if only different values for the intrinsic densities are defined the bandgap's center will be all aligned at the same energy level. Since this is not the general situation for semiconductor hetero structures, we allow the specification of a shift δE_i for the bandgap's center or equivalently of the intrinsic Fermi level E_i. The intrinsic densities n_{in}, n_{ip} in the model (1) are then

$$n_{in} = n_i e^{\delta E_i / V_T}, \quad n_{ip} = n_i e^{-\delta E_i / V_T}. \tag{2}$$

Here, large gradients for the potential ψ and carrier densities $n = n_{in} e^{\psi/V_T}$ and $p = n_{ip} e^{-\psi/V_T}$ are to be expected at the interfaces between different materials, see [1], [3]. Our implementation of the drift-diffusion model allows the parameter n_i, E_i in (2) to be specified as piecewise constant functions since carrier densities are generally discontinuous functions at the interfaces between different materials. The computation of such discontinuous fields should be avoided. The implemented finite element method only computes continuous solutions and a very large number of elements would be necessary to approximate discontinuities. To circumvent this problem, the discretization of the drift-diffusion model is therefore performed with respect to the continuous variables $(\psi, n/n_{in}, p/n_{ip})$. For the numerical results of this model, Fig. 2-3 show the potential field and electron density as computed for the device of Fig. 1.

Although for heterogeneous materials and non-degenerated semiconductors the Poisson equation yields a correct representation of the bandshapes, the current continuity equations based on the linearization of the Boltzmann transport equation may not yield correct current-voltage characteristics. At the interface between two semiconductors with different bandgaps, strong carrier-carrier interactions are present and only Monte Carlo methods are generally able to properly

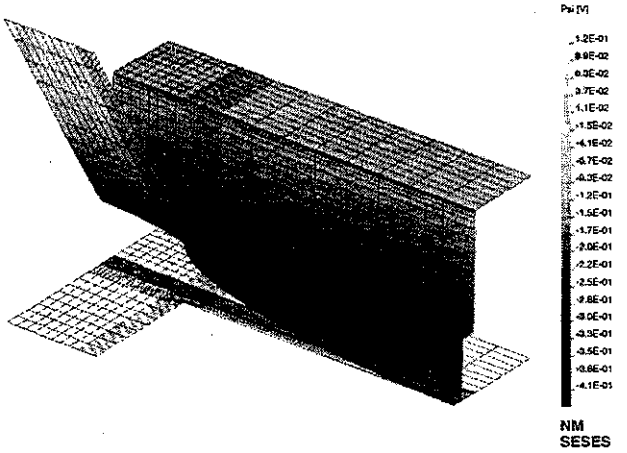

Figure 2: The potential field distribution for one-half of the laser device of Fig. 1.

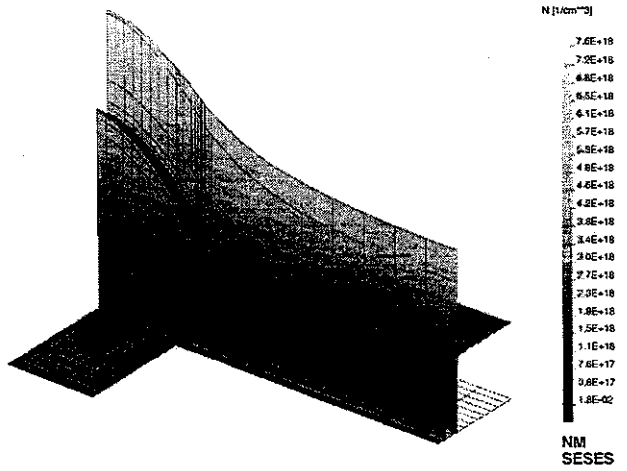

Figure 3: The electron density for one-half of the laser device of Fig. 1.

model the physics. This limitation is probably not the major source of error for modeling the presented laser device. Typically, recombination parameters play a very important role in the approximation process, as for example when determining the lasing condition.

GOVERNING EQUATIONS FOR OPTICAL FIELDS

In the present work, the optical fields are computed as quasi-TE or quasi-TM modes of optical two-dimensional dielectric waveguides propagating along the z-axis. These modes are obtained by solving the scalar Helmholtz problems for the y-component of the electric and magnetic optical field E_y and H_y, using

$$\begin{aligned} &\left[\vec{\nabla}^2 + \left(\tfrac{2\pi n}{\lambda}\right)^2 - (\beta)^2\right] \mathcal{E}_y = 0\,, \\ &E_y = \mathcal{E}_y e^{i(\omega t - \beta z)}\,, \end{aligned} \tag{3}$$

for TE modes, and

$$\begin{aligned} &\left[\vec{\nabla}\tfrac{1}{n^2}\vec{\nabla} + \left(\tfrac{2\pi}{\lambda}\right)^2 - \left(\tfrac{\beta}{n}\right)^2\right] \mathcal{H}_y = 0\,, \\ &H_y = \mathcal{H}_y e^{i(\omega t - \beta z)}\,, \end{aligned} \tag{4}$$

for TM modes, where n is the refractive index, λ the wavelength, $\omega = 2\pi c/\lambda$, and β the eigenvalue representing the mode propagation velocity. For a piecewise constant refractive index with the invariance property $\partial_y n = 0$, the solutions of (3) and (4) yield exact TE and TM solutions of the Maxwell equations, see [15]. In practice, these exact solutions do not exist since the optical mode must be limited laterally in some way. However, if the refractive index variations along the y-axis are small compared to the ones along the x-axis, then the optical modes will preserve the TE and TM character and the solutions of the scalar equations (3), (4) with a y depending refractive index will result in approximate solutions of the Maxwell equations. These solutions are called quasi-TE and quasi-TM modes. For the laser device of Fig. 1, Fig. 4 displays the ground quasi-TE optical mode. The reason why the waveguide modes are computed as quasi-TE or quasi-TM modes relies on the simplicity of the scalar formulation. Solving the Maxwell equations with zero source terms is more complex because of the intrinsic vector character. Here, spurious modes may appear if inadequate discretization methods are used.

COUPLING BETWEEN OPTICAL AND ELECTRIAL FIELDS

Different classes of devices have in general quite different couplings between optical and electrical fields, however, for many devices this coupling can be given

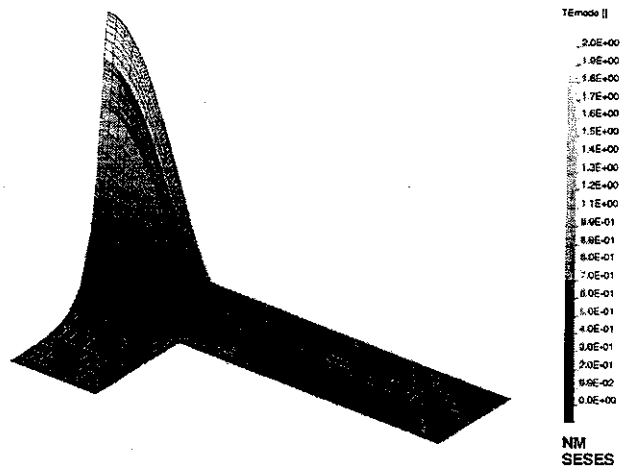

Figure 4: The ground quasi-TE mode of the dielectric waveguide defined by the laser device of Fig. 1. Only one half of the device is shown.

by defining special models for the recombination. In particular, for the laser example in Fig. 1, the coupling is determined by stimulated emission of light given by the relation

$$\begin{aligned} R^{stim} &= gain \times photon\ flux \\ &= gain \times energy\ flux/\hbar\omega\,, \end{aligned} \tag{5}$$

where $g = g(n,p)$ is the material gain. Different gain models are available, which are in general given as polynomials in the variables n and p with coefficients fitted from experimental data. For example, in this implementation the models

$$\begin{aligned} g_1(n,p) = {} & A_0 z + A_1 z^2\,, \\ g_2(n,p) = {} & g_1(n,p) - (C_0 + C_1 z + \\ & C_2 z^2)\left(\lambda - (L_0 - B_0 z - B_1 z^2)\right)^2\,, \end{aligned} \tag{6}$$

are used with $z = \sqrt{np} - N_0$.

The energy flux is evaluated using the relation $energy\ flux = const\ \Phi^2$ where Φ is the computed and normed optical amplitude proportional to E_y or H_y and $const$ is a user defined value expressing the power of the optical beam. This stimulated recombination is then added to other recombination models like Schottky-Read-Hall, spontaneous, and Auger recombination models. The total recombination rate for the laser device in Fig.1 forward biased by 1.4 V and for an optical beam of 10 mW is given in Fig. 5. As for the carrier densities, the recombination rate is also a discontinuous function at the interface between different materials.

NUMERICAL ALGORITHMS

Once the governing equations for the optical and electrical fields are defined and the type of coupling has been specified, numerical methods are applied to solve all of the equations consistently.

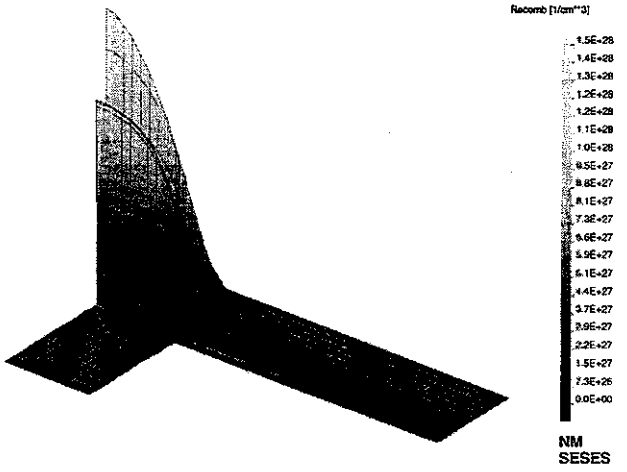

Figure 5: The recombination rate for one-half of the laser device of Fig. 1.

In a first step, one has to consider the type and magnitude of the coupling between the physical fields. For the example in Fig 1, the dynamical behavior when a beam of light traverses the laser device is of primary interest. Since the lateral dimensions of the device are small compared with the longitudinal length, we may perform all numerical computations on a two-dimensional section. Therefore to model this device we proceed as follows.

The user specifies the power of the optical beam entering the device. The scalar Helmholtz equations for TE or TM-modes are then solved to obtain the mode amplitude. The next step is to solve the drift-diffusion model to obtain the electrical fields and to use the mode amplitude to determine the amount of stimulated recombination.

Since the optical modes are computed for a device at rest, i.e. without an optical beam, this solution is not really consistent. Stimulated recombination affects the density of the carriers which in turn affects the refractive index of the dielectric waveguide and thus the optical modes. It is possible to obtain a consistent solution with a Pickard iteration method, thus by restarting the whole solution process with the last computed field values. Since this type of coupling is weak, the convergence is assured in a few iterations and in most cases no iterations at all are required. This is even more true for hetero junction devices where the refractive index differences between film and cladding layers are large.

From the solutions of the drift-diffusion model the amount of stimulated recombination and carrier densities are obtained. These values are first used to compute locally and then globally an averaged gain factor for the mode amplitude. We can now make a small step along the longitudinal z-direction and with the computed averaged gain factor we are able to determine the optical power. With the optical field now given at this new section, the whole computation can be repeated. If this process is repeated for a certain number of sections, at the end we get the beam amplitude at the output of the device.

With a weak coupling mechanism from the electrical towards the optical fields as discussed above, the modeling of this laser device may be characterized as one directional. First one can compute the optical fields and then the electrical fields. This is true for the presented example, but if one uses the laser diode as a self-sustained laser then the coupling becomes bidirectional. Computing solutions for this case is typically more difficult and instabilities related to the existence of multiple solutions may occur for example, when different optical modes are competing. Here we will not further discuss this type of solutions.

Next the numerical algorithms used to solve the governing equations are briefly presented. The scalar Helmholtz equations are discretized with standard rectangular Q_1 finite elements [4]. To find eigenpairs $(\lambda, \vec{x})$ of the generalized eigenproblem $A\vec{x} = \lambda M\vec{x}$ for the positive definite matrices A and M, the Lanczos algorithm is used to compute a subspace consisting of orthogonal vectors and a QR-algorithm with shift diagonalizes the tridiagonal matrix obtained by the Lanczos algorithm as the projection of the original problem onto the subspace [6]. A partial reorthogonalization algorithm is used to keep the Lanczos vectors almost orthogonal to each other [14].

The three equations of the drift-diffusion models are one of type elliptic and two of type parabolic. Following the method of lines we first discretize the space variables and deal with time as a continuous variable. Each single equation of the drift-diffusion model is discretized in space by mixed finite element methods and Q_1 elements [10], [11]. For a successful implementation of this method, it is mandatory to have an exact and fast numerical evaluation of exponentially fitted integrals. These integrals arise when discretizing the electron and hole current continuity equations, see also [12] for further details on the numerical algorithms.

After the discretization of the spatial variables, a system of ordinary differential equations for the time variable is obtained. Because the system can be very stiff, general A-stable methods as the standard second order trapezoidal integration algorithm are not well suited and may lead to unwanted oscillations. Better suited are the so called L-stable methods, like the BDF2 method which has been used together with an adaptive time step selection algorithm [7], [8]. A composite trapezoidal-BDF2 method is also a possible choice and offers some advantages, see [2].

All linear systems arising during the solution process have been solved by LU-factorization and the minimum degree algorithm has been used to minimize the amount

of fill-in during the factorization process [5].

As shown in Figs. 2-5 for steady state solutions of the laser device of Fig. 1, as well as for the unstationary solutions computed, the numerical solutions do not show spurious oscillations and this despite the fact the carrier densities are discontinuous and large gradients are presented in the potential field at the interface between different materials. This good numerical behavior is also reflected by a good convergence behavior of the non-linear Newton-Raphson solution algorithm used to solve the discretized and linearized drift-diffusion model.

COMPUTATIONAL EXAMPLE

The aim of the presented example is to compute the dynamical behavior of a laser diode upon the arrival of an optical signal, see Fig. 6. A large optical control signal is used to change the refractive index of the dielectric waveguide. Here the reduction of carriers inside the active region caused by stimulated recombination induces a change of the refractive index through the plasma effect. If in addition to the control signal a small data signal is added, this latter signal will not affect the state of the device to a first order and the signal will see a change in the refractive index as caused by the control signal. The change of the refractive index will affect the propagation velocity of the data signal inside the waveguide, an effect used for optical switching. Important for this device is a fast recovery when the optical control signal is switched off. Here, the carriers must be swiftly injected to quickly restore the original state and the refractive index of the waveguide.

To study this problem, we have carried out time dependent simulations, where we have only computed solutions at the input facet of the laser device.

In one of the examples, short Gaussian shaped optical signals of 6 *ps* FWHM are injected into the input facet of the laser, see Fig. 7. The response of the laser given by the averaged gain

$$< Gain >= \int g(n,p)\Phi^2 dxdy \qquad (7)$$

is shown in Fig. 8. This averaged gain is directly correlated with the change of the propagation velocity of the data signal. The mobile carrier concentration is quickly reduced because stimulated emission is taking place immediately after arrival of the signal, however, the recovery is a much slower process because of the limited carrier mobility.

CONCLUSIONS

Through an example of a semiconductor laser diode, numerical methods for modeling photonic devices have been presented. If the drift-diffusion model may be considered a general tool for computing the electrical fields, the governing equations for the optical fields and the numerical methods used for their solutions must be chosen according to the class of optical devices being considered. The coupling between optical and electrical fields is in general given by the definition of recombination models although the specification of model parameters is in general not yet available. Numerical solutions without spurious oscillations are obtained with the proposed numerical algorithms implemented with the program NM Seses .

REFERENCES

[1] G. P. AGRAWAL, N. K. DUTTA, *Long-wavelength semiconductor lasers,* Van Nostrand, 1986.

[2] R. E. BANK, W. M. COUGHRAN, W. FICHTNER, E. H. GROSSE, D. J. ROSE, R. K. SMITH, *Transient Simulation of Silicon Device and Circuits,* IEEE Trans. on Computer-aided Design, Vol. CAD-4, No. 4, 1985.

[3] H. C. JR. CASEY, M. B. PANISH, *Heterostructure lasers,* Academic Press, 1978.

[4] P. G. CIARLET, *Basic error estimates for elliptic problems,* Handbook of Numerical Analysis by P.G. Ciarlet and J.L Lions, Volume II, North-Holland, 1991.

[5] A. GEORGE, J. W.H. LIU, *The Evolution of the minimum degree ordering algorithm,* SIAM Review, Vol. 31, No. 1, pp 1-19, 1989.

[6] G. H. GOLUB, C. F. VAN LOAN, *Matrix computations,* Johns Hopkins University Press, 1993.

[7] E. HAIRER, S. P. NORSETT, G. WANNER, *Solving Ordinary Differential Equations I, Nonstiff Problems,* Springer-Verlag, 1993.

[8] E. HAIRER, G. WANNER, *Solving Ordinary Differential Equations II, Stiff and Differential-Algebraic Problems,* Springer-Verlag, 1996.

[9] P. A. MARKOWICH, *The Stationary semiconductor device equations,* Springer-Verlag, 1986.

[10] J. E. ROBERTS, J. M. THOMAS, *Mixed and hybrid methods,* Handbook of Numerical Analysis by P.G. Ciarlet and J.L Lions, Volume II, North-Holland 1991.

[11] G. SARTORIS, *A 3D rectangular mixed finite element method to solve the stationary semiconductor equations.* SIAM J. Sci. Comp., Vol. 19, No. 2, 1998.

[12] G. SARTORIS, *A fast algorithm to compute the moments of the exponential function for application to semiconductor modeling.* COMPEL, Volume 16, No. 1, 1997.

[13] S. SELBERHERR, *Analysis and simulation of semiconductor devices,* Springer-Verlag, 1984.

[14] H. D. SIMON, *The Lanczos Algorithm with partial reorthogonalization,* Math. of Computation, Vol. 42, Num. 166, pp 115-142, 1984.

[15] A. YARIV, *Quantum Electronics,* John Wiley & Sons 1989.

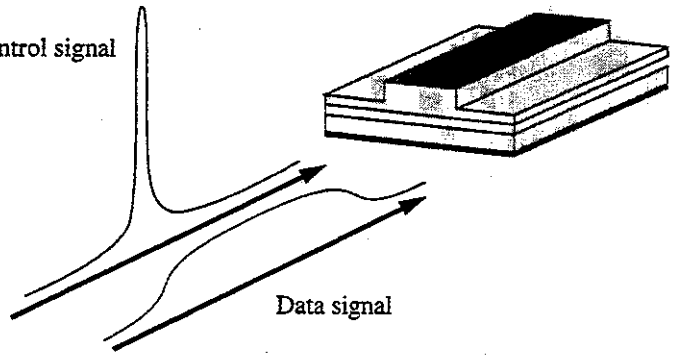

Figure 6: A semiconductor laser device with a control and a data signal. The large control signal is used to induce a change of the effective refractive index for the data signal.

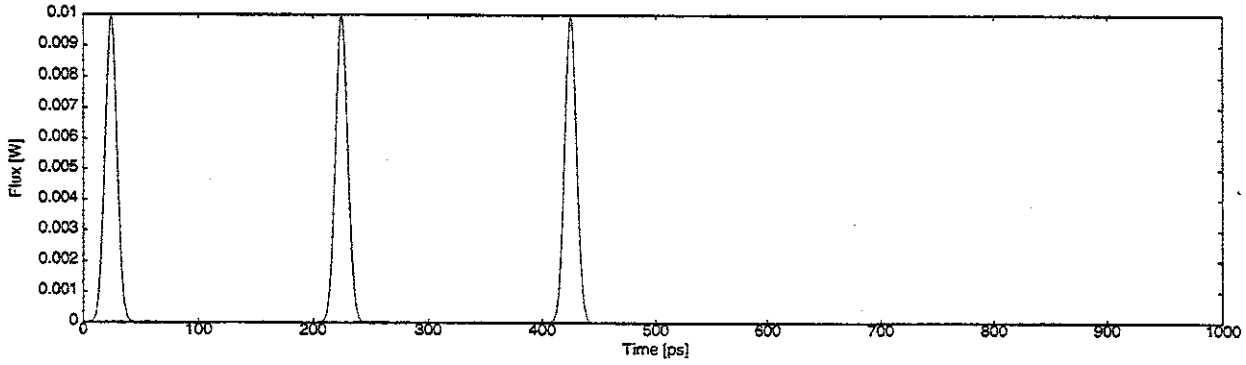

Figure 7: Gaussian shaped optical signals with 6 *ps* FWHM going through the semiconductor laser.

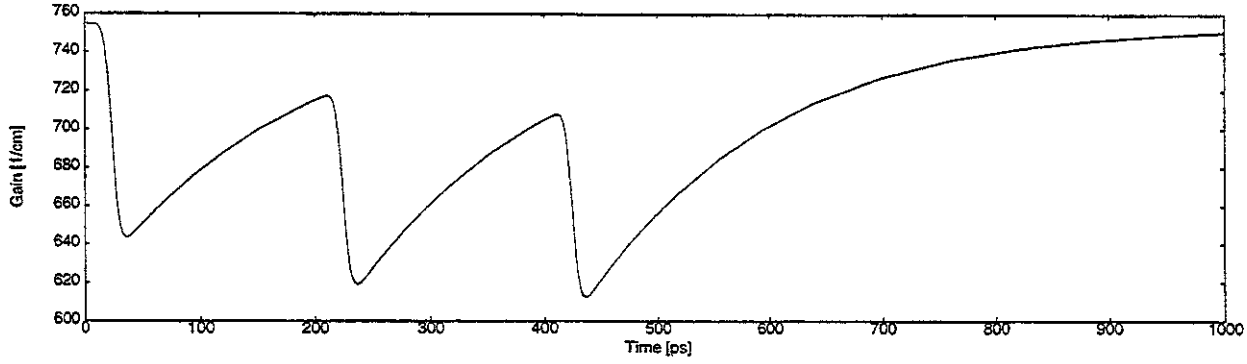

Figure 8: The laser gain response to the optical signal in Fig. 7.